CrystEngComm

Accepted Manuscript

ROYAL SOCIETY OF CHEMISTRY

www.rsc.org/crystengcomm

ARTICLE TYPE www. rsc.org/xxxxxx | XXXXXXXX

Interplay of Ligand Chirality and Metal Configuration in Mononuclear Complexes and in a Coordination Polymer of Cr(III)†

Ai Wang,[a] Carina Merkens,[a] and Ulli Englert*[a]

Received Xth XXXXXXXXXX 20XX, Accepted Xth XXXXXXXXX 20XX
First published on the web Xth XXXXXXXXXX 200X
DOI: 10.1039/b000000x

In order to investigate the influence of ligand chirality on the configuration of the coordinated metal, five pseudooctahedral Cr(III) complexes with one or two chelating *R,R*-1,2-diaminocyclohexane ligands have been synthesized. The mononuclear complexes $[Cr(R,R\text{-chxn})_2Cl(DMSO)]Cl_2$, $[Cr(R,R\text{-chxn})_2Cl_2]Cl$, $[Cr(acacCN)(R,R\text{-chxn})_2](NO_3)_2$, $[Cr(acacCN)_2(R,R\text{-chxn})]NO_3$, $[Cr(acacCN)_2(R,R\text{-chxn})]PF_6$. (*R,R*-chxn = *R,R*-1,2-diaminocyclohexane; acacCN = deprotonated 3-cyanoacetylacetone and DMSO = dimethyl sulfoxide) have been obtained as crystalline solids, mostly solvates, and the potential chirality transfer from the enantiopure ligand to the configuration at the Cr(III) center has been investigated. The cationic complex $[Cr(acacCN)_2(R,R\text{-chxn})]^+$ has been synthesized as exclusively Λ configured at the metal. In this complex, the dangling nitrile groups of the ditopic acacCN ligands may coordinate to Ag(I): the chiral-at-metal building block has thus been converted to the 2D network $Ag[Cr(acacCN)_2(R,R\text{-chxn})]_2(PF_6)_3$ under retention of the stereochemistry at Cr(III). With respect to topology, the polycations in this mixed-metal coordination polymer correspond to two interpenetrated {4,4} nets.

1 Introduction

An object not superimposable with its mirror image is called chiral.[1] Chiral molecules are ubiquitous in living organisms, but chirality is not restricted to biomolecules: chiral materials and coordination compounds which may be obtained in enantiomerically pure form offer attractive potential, e.g. in asymmetric catalysis. Alfred Werner[2], the father of coordination theory, could prove as early as 1907 with the successful resolution of hexol that chirality is not necessarily associated with carbon.[3] Nowadays, it is common knowledge that pseudooctahedral complexes between a metal cation and three bidentate chelating ligands exist as Δ and Λ isomers.

The potentially ditopic molecule 3-cyanoacetylacetone (HacacCN)[4] has been used for crystal engineering purposes. It may be deprotonated to a formally anionic ligand, combining the chelating pentanedionato moiety with an additional N coordination site; it can thus act as a linker in mixed-metal coordination polymers.[5–9] Cr(III) represents a promising candidate for combining metal chirality with crystal engineering, for example, for the construction of chiral extended structures. It is a hard and inert cation for which only slow racemization can be expected. Its acetylacetonate complex has been successfully resolved into enantiomers[10] by using a chiral base as deprotonating agent, followed by recrystallization. We can confirm this earlier report, but our attempts to resolve $Cr(acacCN)_3$ into enantiomers in an analogous way were not successful: we only achieved low enantiomeric excess and very modest yields. An alternative way to induce a well-defined configuration about a metal cation relies on the use of organic ligands and transfer of the chiral information to the metal center.[11–13] The combination of chirality at the metal with an enantiomerically pure ligand results in diastereomers which differ in their physical properties; under favourable conditions, the diastereomer of lower energy may then become the dominant reaction product. We have focussed on the combination of Δ/Λ metal chirality in tris(chelating) pseudooctahedral complexes and *RR* configuration in the chelating ligand *R,R*-1,2-diaminocyclohexane (*R,R*-chxn). The energetic preference for the Δ configuration at the central atom of the octahedral $[M(R,R\text{-chxn})_3]^{3+}$ complex cations was established for M = Co by Harnung and coworkers[14] and is reflected by the fact that this diastereomer represents the readily available main product from crystallization experiments for $[M(R,R\text{-chxn})_3]Cl_3{\cdot}nH_2O$ (M = Co, Rh)[15], $[Cr(R,R\text{-chxn})_3]Cl_3{\cdot}nH_2O$[16] and $[M(R,R\text{-chxn})_3]NO_3{\cdot}nH_2O$[17]. Stoeckli-Evans and coworkers have successfully used enantiopure 1,2-diaminocyclohexane as chirality-inducing constituent in bimetallic assemblies.[18,19] The same enantiopure diamine has been employed in the crystallization-induced resolution of biaryl derivatives.[20] We

† Electronic Supplementary Information (ESI) available: [Crystallographic information in CIF format; details concerning crystallization, structure solution and refinement of **1** - **4** and **6** - **8**; hydrogen bonds interaction of **1**, **2**, **6** and **8**; displacement ellipsoid plots of asymmetric unit for **1** - **4** and **6** - **8**; powder patterns for **1**, **2**, **4**, **5**, **6**, **7** and **8**.]. See DOI: 10.1039/b000000x/

[a] *Institute of Inorganic Chemistry, RWTH Aachen University, Aachen, Germany. Fax: +49 241 8092 288; Tel: +49 241 809 4666; E-mail: ullrich.englert@ac.rwth-aachen.de*

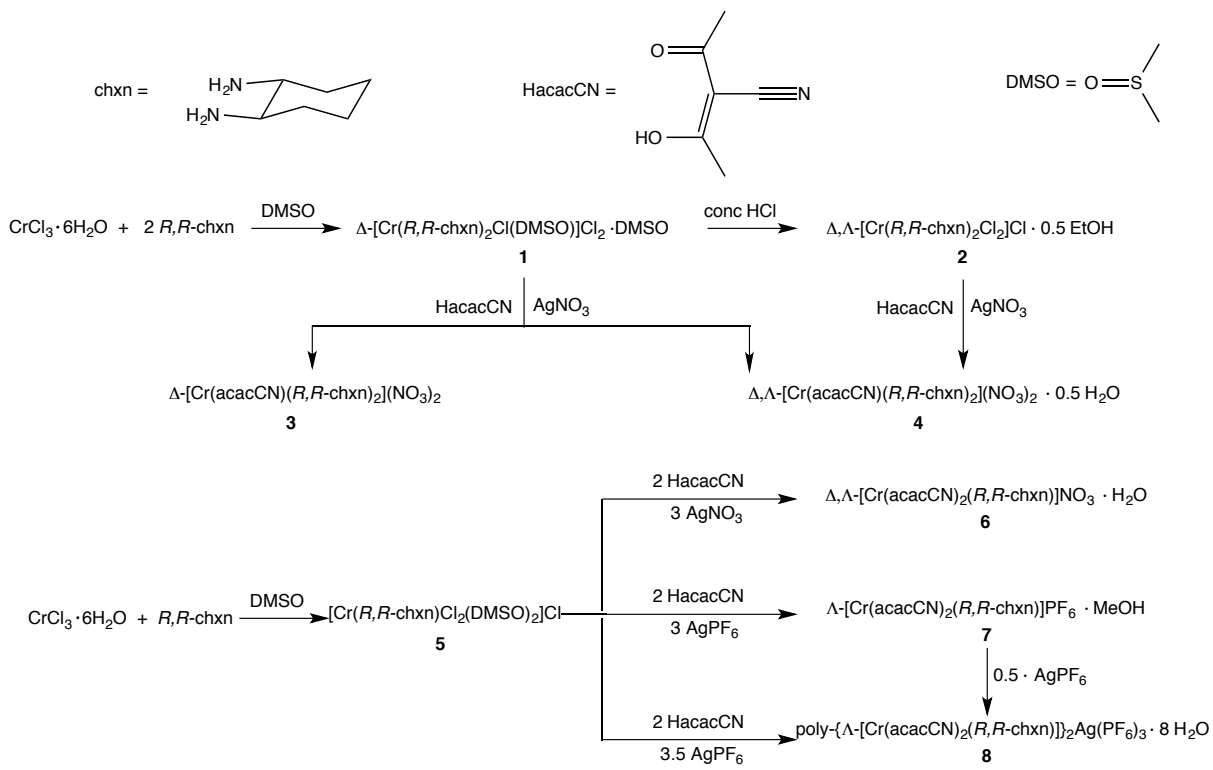

Fig. 1 Scheme of sythesis and naming convention for reactions and crystal structures determined in the context of this work.

shortly mention that not only enantiopure but also racemic 1,2-diaminocyclohexane has been applied in the field of crystal engineering: chxn complexes of transition metals have proven suitable counter cations for thioantimonates[21] and indiumsulfates.[22] As for the enantiopure diaminocyclohexane ligand, we hoped to exploit its central chirality and generate complexes of well-defined metal configuration containing only two or even only one molecule of *R,R*-chxn as a chelating ligand. The cations reported here adopt the composition $[Cr(R,R\text{-chxn})_2L_2]^{n+}$ (L = monodentate ligand, n = 1-2), $[Cr(acacCN)(R,R\text{-chxn})_2]^{2+}$ or $[Cr(acacCN)_2(R,R\text{-chxn})]^{+}$. Our special focus was on the latter complex for an obvious reason: a configurationally well-defined $[Cr(acacCN)_2(R,R\text{-chxn})]^{+}$ cation would represent a chiral-at-metal building block with two additional potential donor sites in the periphery and therefore be suitable for crosslinking to extended structures. The compounds investigated in this context have been summarized in Fig. 1.

2 Results and discussion

We will first address salts in which the cationic Cr(III) complex contains two chelating chxn and two additional monodentate ligands in the coordination sphere. $[Cr(R,R\text{-chxn})_2Cl(DMSO)]Cl_2$ and $[Cr(R,R\text{-chxn})_2Cl_2]Cl$ were synthesized by Pedersen[23] in 1970, but their crystal structures have not yet been reported. We now provide this information: single crystals suitable for diffraction experiments of both compounds could be grown as DMSO solvate of the former (**1**) and EtOH hemisolvate of the latter (**2**) compound (Fig. 1); powder diffraction on the bulk (Figs. S16 and S17, ESI) confirmed that in either case a phase pure product was obtained. Like all solids reported here, these products are derivatives of enantiomerically pure *R,R*-chxn and hence necessarily crystallize in chiral space groups. Both **1** and **2** contain two complex cations per asymmetric unit but differ with respect to the stereochemistry at the metal: the $[Cr(R,R\text{-chxn})_2Cl(DMSO)]^{2+}$ cations in **1** are both Δ configured whereas **2** features one $[Cr(R,R\text{-chxn})_2Cl_2]^{+}$ in Δ and one in Λ configuration. A comment concerning short contacts between discrete residues seems appropriate: in view of the potential donors and acceptors, the existence of conventional hydrogen bonds in **1** and **2** as well as in all other structures reported here is no surprise. In **1**, only the uncoordinated Cl^{-} and DMSO residues accept N-H hydrogen bonds. In contrast to this situation, the hydrogen bonds in **2** cover a wider distance range and both uncoordinated and metal coordinated groups act as acceptors. In both solids **1** and **2**, classical hydrogen bonds

give raise to 2D layer structures. A synopsis of all classical hydrogen bonds in **1**, **2**, **6** and **8** is provided in Table S1 (ESI).

Our next aim was to introduce the ditopic linker HacacCN into the Cr(III) complexes, possibly under control of the configuration at the metal. The reaction was achieved by precipitating the chloride ligands in **1** or **2** with $AgNO_3$ in the presence of the deprotonated acacCN ligand. The main reaction product is Δ, Λ-[Cr(acacCN)(*R,R*-chxn)$_2$]$(NO_3)_2$; it can be isolated as hemihydrate **4**. When the DMSO complex **1** is used as starting material, a second compound **3**, Δ-[Cr(acacCN)(*R,R*-chxn)$_2$]$(NO_3)_2$, is obtained concomitantly. We have been able to elucidate the stereochemistry at the Cr(III) centers in **3** and **4** by single crystal X-ray diffraction: **3** only contains Δ configured cations whereas **4** features complex cations in either configuration. The quantitative relationship between **3** and **4** has been established by powder diffraction of the bulk: Fig. 2 shows that reaction of **2** gives **4** as a phase pure solid, whereas the conversion of **1** results in a mixture in which **3** is present in only small quantities as a by-product. Unfortunately, the main product **4** does not meet our requirements for a single configuration at the metal.

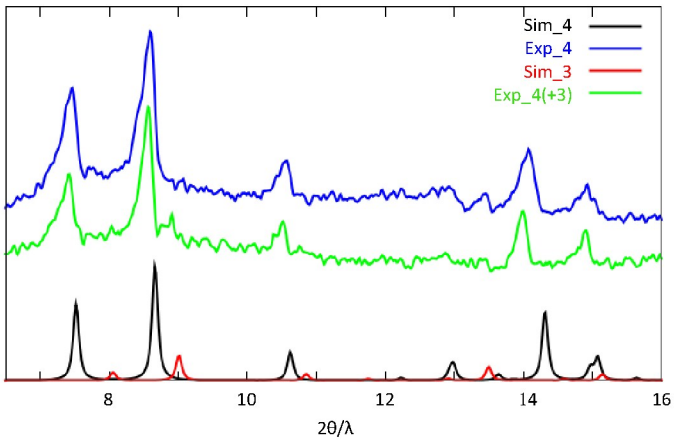

Fig. 2 The powder diffraction pattern of experimental and simulated of **3** and **4**.

4 and its by-product **3** are closely related with respect to packing. Fig. 3 shows projections of both structures along the shortest crystallographic axis. In **3** , classical hydrogen bonds result in layers extending along the diagonal and the short axis - the hydrogen-bonded network is two-dimensional. In **4** , these layers are crosslinked by the additional water molecules in the crystal lattice (highlighted in Fig. 3 bottom); a 3D network of hydrogen bonds is formed. The presence of acacCN in the coordination sphere around Cr in **3** and **4** has another consequence for intermolecular interactions. The peripheral CN groups of the acacCN ligand represent additional potential acceptors for hydrogen bonds; such contacts also occur in 7. Table 1 summarises all classical hydrogen bonds in **3**, **4** and **7**; contacts with nitril acceptors have been highlighted in bold. The table shows that CN···H-N bonds range between 3.0 and 3.1 Å. The only CN···H-O interaction is due to a contact with the hydroxyl group of a cocrystallised MeOH molecule in **7** and is significantly shorter.

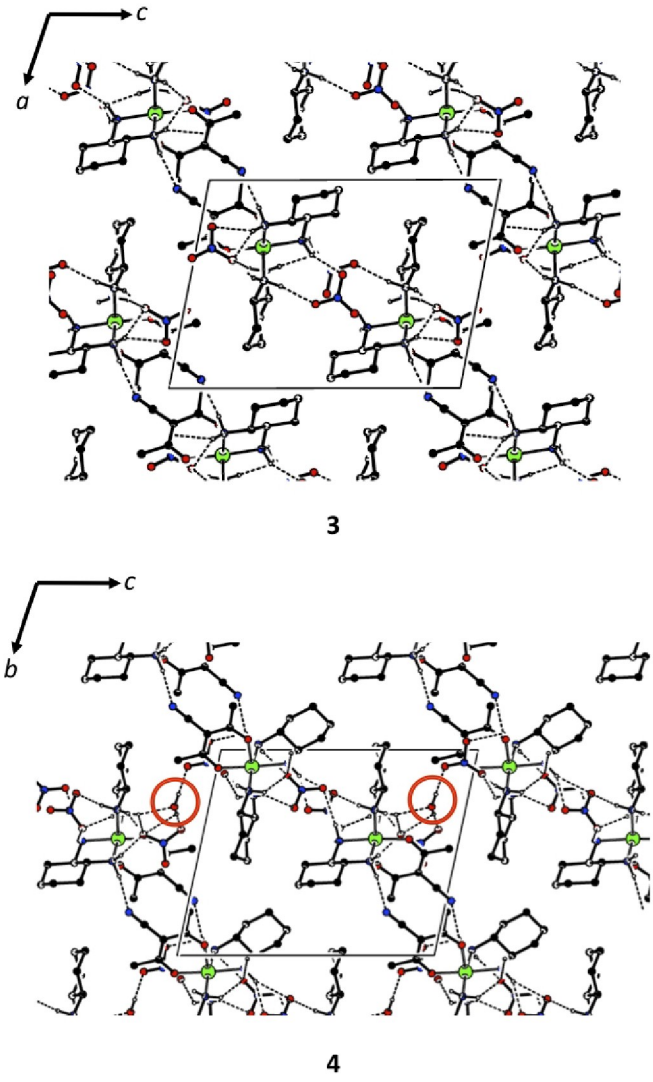

Fig. 3 Hydrogen bonds form layers in **3** (top) which are crosslinked by cocrystallized water molecules in **4** (bottom); the crosslinking water molecules have been highlighted by red circles.

With respect to the stereochemistry at the Cr center, we can summarize our results for **1** - **4**: each Cr(III) in these salts is coordinated to two enantiopure diaminocyclohexane ligands. The cationic Cr complexes either occur in Δ or as a mixture of Δ and Λ configuration - no solid with a preference for a Λ configured cation has been encountered. However: in the crystalline products **2** and **4**, Δ and Λ configuration coexist in 1:1

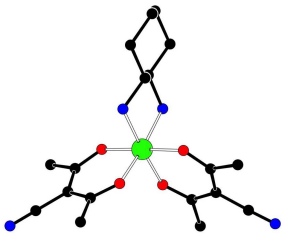

Δ configured cation in **6**

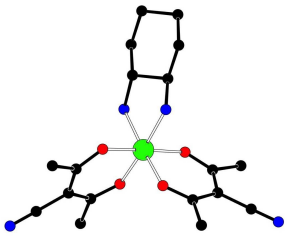

Λ configured cation in **6**

Fig. 4 Δ (left) and Λ (right) configured $[Cr(acacCN)_2(R,R\text{-chxn})]^+$ cations in **6**.

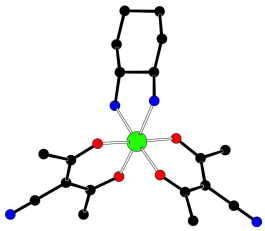

Λ configured cation in **7**

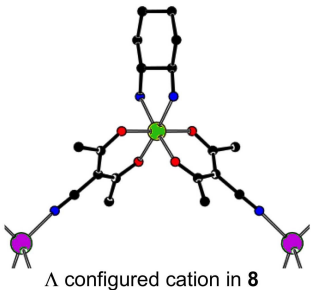

Λ configured cation in **8**

Fig. 5 Λ configuration in the discrete cations in **7** (left) and in the Ag-bridged cations of polymer **8** (right)

stoichiometry, and the concomitantly formed products **3** and **4** do not exhibit the same stereochemistry. These findings suggest that the energetic difference between the diastereomers Δ-metal/*RR*-chxn and Λ-metal/*RR*-chxn is not very pronounced: other structural features such as the nature of the counteranions or the degree of solvation may well be decisive.

From a crystal engineering point of view, **3** and **4** represent dead ends because they offer only one terminal CN function for further coordination. At least two potential linker sites should be available for the construction of an extended solid. We therefore proceeded with the synthesis of the more suitable precursor $[Cr(R,R\text{-chxn})Cl_2(DMSO)_2]Cl$, **5**, which we expected to convert into a building block with two ditopic acacCN ligands. This intermediate can be obtained in reasonable yield and may be characterised by elemental analysis. We have not been able to grow sufficiently large crystals for a full structural study of this compound, but the solubility properties of **5** support its identity as a salt and its reactivity matches the expectation: with silver salts of weakly or non-coordinating anions, the precursor can be converted to salts containing tris(chelated) Cr(III) cations with two ditopic acacCN ligands in the coordination sphere. Repeated powder diffraction experiments showed good internal agreement and thus also confirmed that the synthesis of **5** leads to a reproducible product, albeit with unknown crystal structure.

Based on the intermediate **5**, the nitrate **6** and the hexafluorophosphate **7** have been synthesised and fully characterised. Crystalline **6** is obtained as a rather stable and phase-pure hydrate; the result of the single crystal diffraction experiment matches the powder pattern of the bulk material (Fig. S20, ESI). The unit cell in space group P1 contains four symmetrically independent cationic complexes, two in Δ and Λ. Fig. 4 shows that the overall shape of the cationic complex and the orientation of the chxn ligand in both isomers differ at first sight. As a consequence, packing properties and close contacts such as hydrogen bonds will also differ and affect the free enthalpy of any solid which contains these residues.

7 crystallises as a methanol solvate; larger single crystals may be isolated from the mother liquor and transferred into the cold N_2 stream of the diffractometer whereas crystalline powder shows fast desolvation at room temperature (Fig. S21, ESI). When compared to the earlier reports concerning $M(chxn)_3$ [14–17] and to the structural results for **1** - **4** discussed above, the stereochemistry at the metal in **7** is a surprise: it represents the first solid in which only the Λ configuration is encountered. The above mentioned preference for the Δ-*RR* configuration which was observed in $[M(chxn)_3]^{3+}$ cations and in **1** - **4** with two chxn ligands per metal is obviously no longer valid if only one enantiopure chelating ligand coordinates with the chromium center as in our complexes **6** and **7**. Despite this unexpected stereochemistry, the Λ-$[Cr(acacCN)_2(R,R\text{-chxn})]^+$ cation in **7** matches our original requirements for crystal engineering: it represents a chiral-at-metal building block of defined configuration and allows extension via its two peripheral N donor sites. We recall that Ag(I) represents the preferred acceptor cation for this group;[6,7] Ag(I) was also used as a reagent to precipitate the halide ligands and generate vacant coordination sites at the Cr(III) precursor. Therefore a change in stoichiometry was sufficient to convert **5** into a polymer. Its hydrate **8** has been successfully studied by single crystal diffraction. Fig. 5 shows that the metal configuration has been retained and Cr(III) in **8** is exclusively Λ configured, similar to the situation in **7**.

With a focus on crystal engineering, **8** represents the target solid of this study, constructed by bridging configurationally well-defined $[Cr(acacCN)_2(R,R\text{-chxn})]^+$ cations with Ag(I). PF_6^- counter anions and hydrate water molecules occupy the voids in the resulting cationic framework. Each Λ-$[Cr(acacCN)_2(R,R\text{-chxn})]^+$ building block is linked to two silver cations with its nitrile groups, and in agreement with the Cr:Ag = 2:1 stoichiometry, each Ag(I) is four-coordinated by cyano-N atoms of four different complex cations. The coordination sphere corresponds to an only slightly distorted tetrahedron, with N-Ag-N angles ranging between 99 and 123 °. The program GTECS3D [24,25] [GTECS3D is available free of charge for download from www.gtecs.rwth-aachen.de.] has been used to analyze the topology of the cationic framework in

8. When the [Cr(acacaCN)$_2$(*R,R*-chxn)] complexes are taken as linkers and the Ag(I) cations as four-connected nodes, a {4,4} net (Fig. 6, top) is obtained. Two such nets interpenetrate[26] in the crystal structure of **8** as becomes obvious after suitable simplification of the linkers (Fig. 6, bottom).

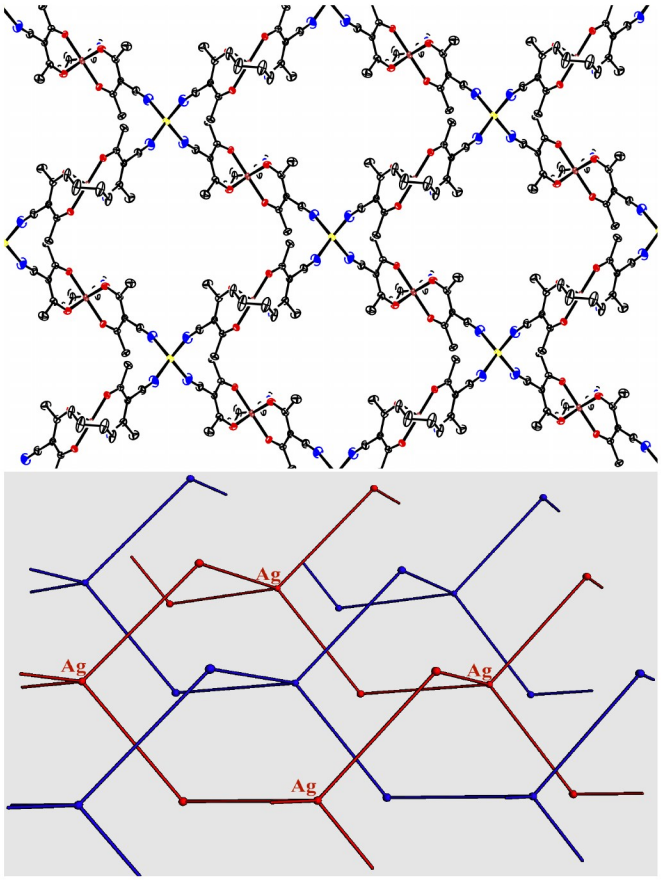

Fig. 6 Section of **8**: {4,4} net formed by [AgCr(acacCN)$_2$(*R,R*-chxn)]$_2$ polycations (top); two such networks interpenetrate in the crystal structure of **8** (bottom).

3 Experimental Section

3.1 Materials and Methods

Enantiopure (*R,R*-chxn) was obtained according to the method of Jacobsen *et al.*[27] The HacacCN ligand was prepared according to the literature method by Silvernail *et al.*;[4] the final purification was made by sublimation. Complexes **1** and **2** were synthesized according to the procedure reported by Pedersen.[23] Other chemicals were used without further purification: $CrCl_3 \cdot 6H_2O$ (98%, Grüssing), $NaHCO_3$ (99.5%, KMF Laborchemie), $AgPF_6$ (98%, Aldrich) and $AgNO_3$ (99.5%, Fluka Chemie). IR spectra were recorded on a Nicolet Avatar 360 E.S.P. spectrometer in KBr pellets. In order to exclude artefacts by reaction of the silver-containing products with KBr, comparisons with IR spectra in nujol mulls were made; they gave satisfactory agreement. CHN microanalyses were carried out at the Institute of Organic Chemistry, RWTH Aachen University, using a HERAEUS CHNO-Rapid. Powder diffraction experiments were performed at room temperature on flat samples with a Stoe & Cie STADI P diffractometer equipped with an imageplate detector with constant ω angle of 55° using germanium- monochromated Cu-$K_{\alpha 1}$ radiation (λ = 1.54051 Å).

3.2 Synthesis

3.2.1 Synthesis of {[Cr(acacCN)(*R,R*-chxn)$_2$](NO$_3$)$_2$}, 3 and {[Cr(acacCN)(*R,R*-chxn)$_2$](NO$_3$)$_2$·0.5H$_2$O}, 4. 27 mg (0.22 mmol) HacacCN and 18 mg (0.22 mmol) $NaHCO_3$ were completely dissolved in 15 ml H_2O. 100 mg (0.22 mmol) **1** were added and the solution turned purple. 112 mg (0.66 mmol) $AgNO_3$ in 3 mL of water were added dropwise, and stirred for 16 hours at room temperature. The precipitate was removed by filtration, the clear solution was evaporated and the residue was dried in a desiccator. The raw product is an orange solid, which was purified by recrystallization from water. Yield: 120 mg (0.23 mmol, 53%). Powder diffraction (see Fig. 2) shows that the reaction product mainly consists of **4**, with a small amount of **3** as byproduct.

3.2.2 Synthesis of {[Cr(acacCN)(*R,R*-chxn)$_2$](NO$_3$)$_2$·0.5H$_2$O}, 4. 16 mg (0.13 mmol) HacacCN and 11 mg (0.13 mmol) $NaHCO_3$ were completely dissolved in 5 ml H_2O. Then 50 mg (0.13 mmol) **2** were added, and the solution turned purple. 66 mg (0.39 mmol) $AgNO_3$ in 5 mL of water were added dropwise, and stirred for 16 hours at room temperature. The precipitate was removed by filtration, the clear solution was evaporated under vacuum and the residue was dried in a desiccator. The raw product is an orange solid, which was purified by recrystallization from water. Yield: 31 mg (0.06 mmol, 47%). The product systematically gives a too low carbon content in elemental analysis, but the powder pattern of the bulk matches the simulation based on the single crystal structure (ESI, Fig. S7 and S8). IR: υ(C≡N, cm^{-1}) = 2216.

3.2.3 Synthesis of {[Cr(*R,R*-chxn)Cl$_2$(DMSO)$_2$](Cl)}, 5. The synthesis of **5** was carried out in analogy to the method by Pedersen[23], but with different stoichiometry. 2.333 g $CrCl_3 \cdot 6H_2O$ (8.76 mmol) were dissolved in 15 mL dimethylsulfoxide (DMSO) and heated to 180 °C to remove the water. After cooling to 110 °C, 1.000 g *R,R*-chxn (8.76 mmol) in 5 mL DMSO was added. A few minutes later, a silky red powder started to precipitate. The reaction was kept at 100 °C for 1 hour and then allowed to cool to room temperature;

the product was precipitated with 150 mL EtOH. This crude product was filtered, washed with EtOH and dried in a desiccator. Yield: 1.941 g (4.53 mmol, 52%). Anal. calcd for **5** [$C_{10}H_{26}Cl_3CrN_2O_2S_2$]: C, 28.01; H, 6.11; N, 6.56. Found: C, 28.28; H, 6.15; N, 7.56.

3.2.4 Synthesis of {[Cr(acacCN)$_2$(*R,R*-chxn)](NO$_3$)·H$_2$O}, 6. 117 mg (0.94 mmol) HacacCN and 78 mg (0.94 mmol) $NaHCO_3$ were added to 5 mL MeOH under stirring. After complete dissolution 200 mg (0.47 mmol) of **5** in 5 mL of water were added. 238 mg (1.41 mmol) of $AgNO_3$ in 5 mL of water were added to the purple solution dropwise and stirred for 16 hours at room temperature. The precipitate was removed by decanting and filtration; the clear red solution was stored at room temperature and allowed to evaporate slowly. After four weeks, the raw product was obtained. Single crystal were grown by recrystallization from MeOH solvent. Yield: 102 mg (0.21 mmol, 44%). Anal. calcd for **6** [$C_{18}H_{28}CrN_5O_8$]: C, 43.73; H, 5.71; N, 14.16. Found: C, 45.53; H, 5.74; N, 13.73. IR: υ(C≡N, cm^{-1}) = 2212.

3.2.5 Synthesis of {[Cr(acacCN)$_2$(*R,R*-chxn)](PF$_6$)·MeOH}, 7. 100 mg (0.23 mmol) of **5** were dissolved in 5 mL MeOH and stirred for 5 min. 58 mg (0.46 mmol) of HacacCN and 39 mg (0.46 mmol) of $NaHCO_3$ were completely dissolved in a mixture of 2 mL water and 5 mL MeOH. Both solutions were combined; after stirring for 20 min, the reaction mixture turned purple. 177 mg (0.70 mmol) of $AgPF_6$ in 5 mL MeOH were added dropwise. Stirring was continued at room temperature for 8 hrs, and then the precipitate was separated by centrifugation. Even after prolonged reaction times, very small amounts of AgCl continued to precipitate and prevent crystallization of the target product; therefore, the clear solution was exposed for 18 hours to UV radiation (λ = 366 nm) in order to remove traces of Ag(I) in solution. The black Ag thus formed was removed by filtration, and the clear red solution was allowed to evaporate at ambient temperature. Red block-shaped crystals formed after 3d. Yield: 44 mg (0.08 mmol, 34%). Anal. calcd for **7** without MeOH [$C_{18}H_{26}F_6CrN_4O_4P$]: C, 38.68; H, 4.68; N, 10.02. Found: C, 38.55; H, 4.65; N, 10.03. IR: υ(C≡N, cm^{-1}) = 2212; υ(P-F, cm^{-1}) = 722.

3.2.6 Synthesis of {Λ-[Cr(acacCN)$_2$(*R,R*-chxn)]$_2$Ag(PF$_6$)$_3$·8H$_2$O}, 8. 100 mg (0.23 mmol) of **5** were dissolved in 5 mL MeOH and stirred for 5 min. 58 mg (0.46 mmol) of HacacCN and 39 mg (0.46 mmol) of $NaHCO_3$ were completely dissolved in a mixture of 2 mL water and 5 mL MeOH. Both solutions were combined; after stirring for 20 min, the reaction mixture turned purple. 177 mg (0.70 mmol) of $AgPF_6$ in 5 mL MeOH were added dropwise. Stirring was continued at room temperature for 8 hrs, and then the precipitate was separated by centrifugation. As in the case of **7**, the solution was exposed for 18 hours to UV radiation (λ = 366 nm) to remove traces of Ag(I), and the black Ag thus formed was removed by filtration. The clear red filtrate and a solution of 30 mg (0.12 mmol) $AgPF_6$ in 3 mL MeOH were combined, and the resulting mixture was kept at room temperature in the dark. After 3d, a small quantity of red plate-shaped crystals were harvested. Yield: 35 mg (0.05 mmol, 20%). Anal. calcd for **8** [$C_{18}H_{34}F_9CrN_4O_8P_{1.5}$·0.5Ag]: C, 28.53 ; H, 4.52 ; N, 7.39. Found: C, 27.11; H, 3.80 ; N, 6.74. IR: υ(C≡N, cm^{-1}) = 2217 with shoulder at 2231; υ(P-F, cm^{-1}) = 722.

3.3 Crystallographic Studies

All intensity data were collected at 100 K on a Bruker D8 goniometer equipped with an APEX CCD area detector and an Incoatec microsource using Mo Kalpha radiation (λ = 0.71073 A). Constant temperature was maintained by an Oxford Cryosystems 700 controller. The intensity data were integrated using the program *SAINT +*[28] and corrected for absorption by multi-scan methods with SADABS.[29] The structures were solved by direct methods (SHELXS-13)[30] and refined by full matrix least square procedures based on F^2 (SHELXL-13)[31]. Non-hydrogen atoms were refined with anisotropic displacement parameters. Hydrogen atoms connected to carbon atoms were placed in idealized positions and included as riding. Tables 2 and 3 contain crystal data, data collection parameters and convergence results. Details about disorder treatment and refinement of H atoms bonded to hetero atoms have been compiled in the ESI. The final structure models are available in CIF format, CCDC number 1047808 - 1047811(**1** - **4**) and 1047812 - 1047814(**6** - **8**).

4 Conclusions

Starting from an enantiopure ligand such as *R,R*-1,2-diaminocyclohexane, the synthesis of chiral solids is a trivial task. Transfer of ligand chirality to the configuration of the central cation is less obvious. Are we telling a success story? With respect to our initial focus, an affirmative answer can be given: making use of the chiral information from the enantiopure ligand, we have been able to synthesize a chiral-at-metal cationic building block [Cr(acacCN)$_2$(*R,R*-chxn)]$^+$ and a related coordination network.The stereochemistry in these target solids is consistent, in agreement with the idea that the configuration once achieved for such an inert complex should be maintained upon further crosslinking even if the resulting coordination polymer should not correspond to the thermodynamically most stable product. With respect to chirality transfer within a building block and crystal engineering of an extended solid, our approach was successful.

And yet we encountered the unexpected: the configuration at the metal in $[Cr(acacCN)_2(R,R\text{-chxn})]^+$ can not be predicted by simple extrapolation from $[Cr(R,R\text{-chxn})_3]^{3+}$ via cationic $[Cr(acacCN)(R,R\text{-chxn})_2]^{2+}$ complexes. The enantiopure ligand and the alternative Δ and Λ configurations at the center of coordination result in diastereomers. These diastereomers in principal differ in energy, but the synopsis of our structural results indicates that the associated energy differences are modest. The energy of a building block obviously does not represent the decisive quantity for the outcome of a crystallisation experiment: interionic Coulomb forces, hydrogen bonds and ubiquituous weaker interactions also contribute to the free enthalpy of the product solids and may well overcompensate the effect of a slightly less favourable diastereomeric complex cation. Fig. 4 shows that the alternative diastereomers differ in shape, charge distribution and orientation of potential hydrogen bond donors and acceptors. Future work will therefore be devoted to understand the role of the remaining constituents, in particular the counteranions engaged in the doubtlessly relevant electrostatic interactions. The direct comparison between the stereochemistry in **6** and **7** suggests that they may be decisive for the configuration at the Cr(III) cation.

5 Acknowledgement

Financial support by China Scholarship Council (A. W.) and RWTH Graduiertenförderung (C. M.) are gratefully acknowledged.

References

1 E. L. Eliel and S. H. Wilen, *Stereochemistry of organic compounds*, John Wiley & Sons: New York, 1993.
2 E. B. Bauer, *Chem. Soc. Rev.*, 2012, **41**, 3153–3167.
3 E. Z. A. Werner, E. Berl and B. G. Jantsch, *Dtsch. Chem. Ges.*, 1907, **40**, 2103–2125.
4 C. Silvernail, G. Yap, R. Sommer, A. Rheingold, V. Day and J. Belot, *Polyhedron*, 2001, **20**, 3113–3117.
5 A. D. Burrows, K. Cassar, M. F. Mahon and J. E. Warren, *Dalton Trans.*, 2007, 2499–2509.
6 M. Kondracka and U. Englert, *Inorg. Chem.*, 2008, **47**, 10246–10257.
7 C. Merkens, N. Becker, K. Lamberts and U. Englert, *Dalton Trans.*, 2012, **41**, 8594–8599.
8 C. Merkens and U. Englert, *Dalton Trans.*, 2012, **41**, 4664–4673.
9 C. Merkens, O. Pecher, F. Steuber, S. Eisenhut, A. Görne, F. Haarmann and U. Englert, *Z. anorg. allg. Chem.*, 2013, **639**, 340–346.
10 S. F. Mason, R. D. Peacock and T. Prosperi, *J. Chem. Soc., Dalton Trans.*, 1977, 702–704.
11 U. Knof and A. von Zelewsky, *Angew. Chem. Int. Ed.*, 1999, **38**, 302–322.
12 J. Crassous, *Chem. Soc. Rev.*, 2009, **38**, 830–845.
13 J. Crassous, *Chem. Commun.*, 2012, **48**, 9687–9695.
14 S. Harnung, B. Soendergaard Soerensen, I. Creaser, H. Maegaard, U. Pfenninger and C. Schäffer, *Inorg. Chem.*, 1976, **15**, 2123–2126.
15 M. Ito, F. Marumo and Y. Saito, *Acta Crystallogr. Sect. B*, 1971, **27**, 2187–2195.
16 I. Kalf, B. Calmuschi and U. Englert, *CrystEngComm.*, 2002, **4**, 548–551.
17 M. Morooka, S. Ohba and H. Miyamae, *Acta Crystallogr., Sect B*, 1992, **48**, 667–672.
18 O. Sereda, A. Neels, F. Stoeckli and H. Stoeckli-Evans, *Cryst. Growth Des.*, 2008, **8**, 3380–3384.
19 O. Sereda, H. Stoeckli-Evans, O. Dolomanov, Y. Filinchuk and P. Pattison, *Cryst. Growth Des.*, 2009, **9**, 3168–3176.
20 H. Degenbeck, A.-S. Felten, J. Etxebarria, E. Escudero-Adan, J. Benet-Buchholz and A. Vidal-Ferran, *Cryst. Growth Des.*, 2012, **12**, 2719–2723.
21 L. Engelke, C. Näther, P. Leisner and W. Bensch, *Z. Anorg. Allg. Chem.*, 2008, **634**, 2959–2965.
22 Y.-H. Wang, J.-B. Jiang, P. Wang, X.-L. Sun, Q.-Y. Zhu and J. Dai, *CrystEngComm.*, 2013, **15**, 6040–6045.
23 E. Pedersen, *Acta Chemica Scandinavica*, 1970, **24**, 3362–3372.
24 K. Lamberts, S. Porsche, B. Hentschel, T. Kuhlen and U. Englert, *CrystEngComm.*, 2014, **16**, 3305–3311.
25 K. Lamberts, C. Merkens, R. Wang, U. Englert, D. Hons, S. Grüter, Y. Guo, S. Porsche, A. Hamacher, D. Bündgens and T. Kuhlen, *Z. Kristallogr. Suppl.*, 2012, **32**, 117.
26 L. Carlucci, G. Ciani, D. M. Proserpio, T. G. Mitina and V. A. Blatov, *Chem. Rev.*, 2014, **114**, 7557–7580.
27 J. F. Larrow, E. N. Jacobsen, Y. Gao, Y. Hong, X. Nie and C. M. Zepp, *J. Org. Chem.*, 1994, **59**, 1939–1942.
28 *SAINT+*. (*Version7.68.*), *Program for Reduction of Data Collected on Bruker CCD Area Detector Diffractometer*, 2009.
29 G. M. Sheldrick, *SADABS (version2.03). A Program for Empirical Absorption Correction, University of Göttingen, Germany*, 2004.
30 G. M. Sheldrick, *Acta Crystallogr., Sect A*, 2008, **64**, 112–122.
31 G. M. Sheldrick, *Acta Crystallogr., Sect C*, 2015, **71**, 3–8.

Table 1 Table 1 Classical hydrogen bonds (Å, °) of **3**, **4** and **7**, contacts involving peripheral CN acceptors have been highlighted in bold.

Comp.	D-H···A	D-H	H···A	D···A	∠D-H···A	Symmetry-for-A
3	N1-H1D···O8A	0.98(5)	2.06(5)	2.975(11)	154(4)	1-x,-1/2+y,1-z
	N1-H1E···O6	0.98(3)	2.02(3)	2.894(7)	147(5)	
	N2-H2D···N5	**0.98(4)**	**2.14(4)**	**3.096(7)**	**165(5)**	**-x, -1/2+y,-z**
	N2-H2E···O4	0.99(5)	2.16(5)	3.042(6)	148(4)	-x,-1/2+y,-z
	N2-H2E···O5	0.99(5)	2.25(5)	2.999(6)	131(4)	-x,-1/2+y,-z
	N3-H3D···O4	0.99(4)	2.00(5)	2.868(6)	146(4)	-x, 1/2+y,-z
	N3-H3E···O6	0.99(5)	2.03(5)	2.943(6)	153(4)	
	N4-H4D···O7A	0.99(3)	2.14(3)	2.993(10)	144(5)	1-x,-1/2+y,1-z
	N4-H4E···O4	0.98(4)	2.13(5)	3.065(6)	158(6)	-x,-1/2+y,-z
4	N1-H1D···O12	0.98(3)	2.44(4)	3.329(8)	151(4)	
	N1-H1E···O6	0.98(4)	2.05(4)	2.966(7)	156(4)	
	N2-H2D···O6	0.98(3)	2.32(5)	2.897(7)	117(4)	-1+x,y,z
	N2-H2D···O17	0.98(3)	2.10(3)	3.007(9)	153(5)	-1+x,y,z
	N2-H2E···O11	0.98(5)	2.00(5)	2.901(8)	153(4)	-1+x,y,z
	N3-H3D···O16A	0.99(3)	2.23(3)	3.204(10)	168(4)	
	N3-H3E···O11	0.99(4)	2.01(4)	2.863(7)	143(4)	-1+x,y,z
	N4-H4D···N10	0.99(3)	2.14(3)	3.124(7)	170(4)	x,1+y,1+z
	N4-H4E···O6	0.98(4)	2.03(5)	2.962(7)	157(4)	
	N6-H6D···O9	0.98(3)	2.37(4)	3.016(7)	123(3)	-1+x,y,z
	N6-H6E···O14A	0.97(4)	2.12(3)	3.015(10)	153(3)	
	N7-H7D···O15A	0.98(3)	2.13(4)	2.965(9)	142(4)	1+x,y,z
	N7-H7E···O9	0.98(4)	1.91(4)	2.863(7)	163(3)	
	N8-H8D···O15A	0.98(4)	2.56(4)	3.076(9)	113(3)	1+x,y,z
	N8-H8E···O12	0.97(3)	2.36(3)	3.266(7)	154(4)	
	N8-H8E···O13	0.97(3)	2.07(4)	2.939(6)	148(3)	
	N9-H9D···O15A	0.97(4)	2.44(4)	3.327(9)	152(3)	
	N9-H9E···O10	0.99(3)	2.35(4)	3.067(7)	128(3)	-1+x,y,z
	N9-H9E···N5	**0.99(3)**	**2.28(4)**	**3.070(7)**	**136(3)**	**x,-1+y,-1+z**
	O1-H17···O6	0.84	2.57	3.117(9)	123	
	O1-H17···O7	0.84	1.79	2.632(12)	180	
	O1-H17···O8	0.85	1.90	2.747(9)	180	x,y,1+z
7	N1-H1D···O5	0.98(3)	2.02(3)	2.966(5)	163(4)	1-x,1/2+y,1/2-z
	N1-H1E···F1	0.97(3)	2.32(4)	3.181(4)	148(3)	1-x,1/2+y,1/2-z
	N1-H1E···F5	0.97(3)	2.10(2)	2.986(4)	151(3)	1-x,1/2+y,1/2-z
	N2-H2D···F3	0.98(3)	2.30(3)	3.189(4)	150(3)	-1+x,y,z
	N2-H2D···F4	0.98(3)	2.40(3)	2.890(4)	110(2)	-1+x,y,z
	N2-H2E···F4	0.98(3)	2.50(3)	2.890(4)	104(2)	-1+x,y,z
	N2-H2E···N4	**0.98(3)**	**2.06(2)**	**3.020(5)**	**163(3)**	**-1/2+x,1/2-y,1-z**
	O5-H5O···N3	**0.72(6)**	**2.15(6)**	**2.858(5)**	**167(7)**	**1/2+x,1/2-y,-z**

Table 2 Crystal data and refinement results of the **1**. **2**. **3** and **4**

Structure	**1**	**2**	**3**	**4**
Empirical formula	$C_{16}H_{40}Cl_3CrN_4O_2S_2$	$C_{26}H_{61}Cl_6Cr_2N_8O$	$C_{18}H_{34}CrN_7O_8$	$C_{36}H_{70}Cr_2N_7O_{17}$
Molecular weight	464.87	815.20	528.19	1074.38
Z	4	4	2	1
cryst. system	monoclinic	monoclinic	monoclinic	triclinic
space group	$P2_1$	$C2$	$P2_1$	$P1$
a (Å)	11.9663(17)	25.314(6)	11.171(4)	7.1767(5)
b (Å)	9.6417(14)	11.006(3)	7.283(2)	12.5519(9)
c (Å)	23.758(3)	14.816(4)	15.335(5)	14.7649(10)
α (°)				100.4860(11)
β (°)	99.533(2)	111.163(5)	101.113(5)	93.4647(11)
γ (°)				106.3580(11)
V(Å^3)	2703.2(7)	3849.6(16)	1224.3(7)	1246.06(15)
Total/unique reflections	32572/11177	16862/7551	18562/7057	19348/14018
R_1 (all data)	0.0468	0.1095	0.0712	0.0645
$R[F^2 > 2\sigma(F^2)]$	0.0378	0.0676	0.0638	0.0538
$(sin\theta/\lambda)_{max}$ (Å^{-1})	0.61	0.59	0.71	0.73
wR_2	0.0880	0.1451	0.1646	0.1277
GOF	1.085	1.001	1.083	1.082
No. of parameters	561	435	322	691
Flack parameter	0.00(2)	0.08(4)	0.03(3)	0.01(2)
CCDC	1047808	1047809	1047810	1047811

Table 3 Crystal data and refinement results of the **6**. **7** and **8**

Structure	**6**	**7**	**8**
Empirical formula	$C_{18}H_{28}CrN_5O_8$	$C_{19}H_{30}CrF_6N_4O_5P$	$C_{36}H_{68}AgCr_2F_{18}N_8O_{16}P_3$
Molecular weight	494.45	591.44	1516.02
Z	4	4	2
cryst. system	triclinic	orthorhombic	orthorhombic
space group	$P1$	$P2_12_12_1$	$C222$
a (Å)	9.5030(6)	8.2870(17)	10.078(2)
b (Å)	13.7410(9)	14.806(3)	42.812(9)
c (Å)	19.6128(13)	21.367(4)	7.2997(16)
α (°)	71.2181(11)		
β (°)	83.8466(12)		
γ (°)	71.8161(11)		
V(Å^3)	2303.2(3)	2621.7(9)	3149.6(12)
Total/unique reflections	36098/26058	36241/7216	238881/4682
R_1 (all data)	0.0645	0.0577	0.0743
$R[F^2 > 2\sigma(F^2)]$	0.0512	0.0451	0.0622
$(sin\theta/\lambda)_{max}$ (Å^{-1})	0.72	0.71	0.72
wR_2	0.1044	0.1044	0.1747
GOF	1.000	1.051	1.087
No. of parameters	1225	345	224
Flack parameter	0.003(7)	-0.002(14)	0.018(14)
CCDC	1047812	1047813	1047814

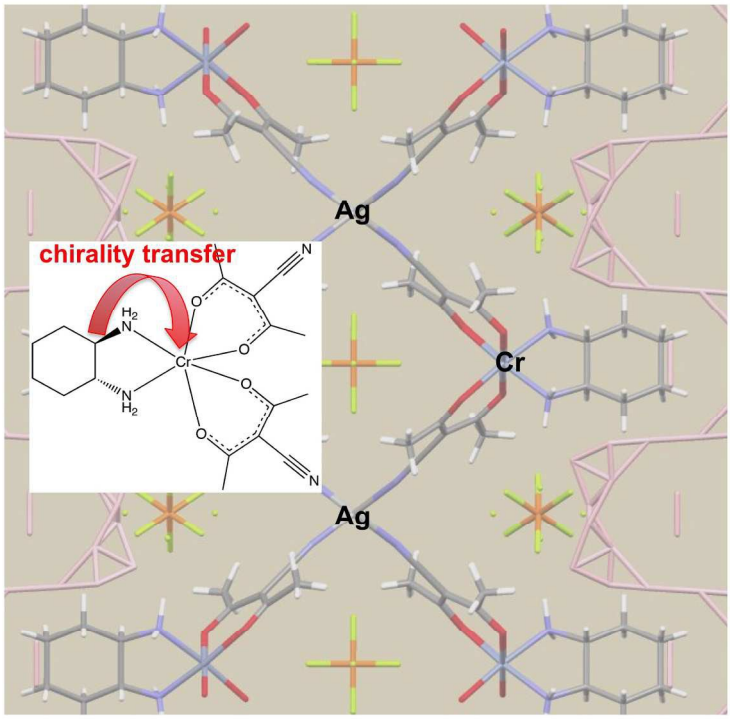

Chiral information may be transferred from a ligand to the coordinated chromium cation. The resulting complex can be crosslinked with a Ag(I) salt to a mixed-metal polymer with well-defined configuration at the Cr(III).
1057x793mm (72 x 72 DPI)